

## Microstructure of quenched Ni-rich Ni-Ti shape memory alloys

Ch. Somsen, J. Kästner, E.F. Wassermann, Ph. Boullay<sup>1</sup> and D. Schryvers<sup>1</sup>

Labor für Experimentelle Tieftemperaturphysik, Gerhard Mercator Universität, Lotharstrasse 1, 47057 Duisburg, Germany

<sup>1</sup> EMAT, University of Antwerp, Groenenborgerlaan 171, 2020 Antwerp, Belgium

Microstructural investigations with transmission electron microscopy were carried out on quenched Ni-Ti alloys with 52 and 54.5 at% Ni. For the  $\text{Ni}_{52}\text{Ti}_{48}$  specimen long time exposed diffraction patterns of a single grain show besides the expected reflections of the B2-phase, two sets of extra reflections in different zones. The first type of spots is explained by lattice displacement waves, which are regarded as precursors of the martensitic Ni-Ti phases, B19' and R-phase, respectively. The second set of reflection with more diffuse intensity than the other reflections is related to  $\text{Ni}_4\text{Ti}_3$  precipitates in an early state of formation. For the Ni-richer  $\text{Ni}_{54.5}\text{Ti}_{45.5}$  alloy only  $\text{Ni}_4\text{Ti}_3$  precipitates in an early state of formation are found but no precursors of the B19'- and R-phase.

### Introduction

Ni-Ti shape memory alloys show martensitic phase transitions from the parent B2-phase (CsCl-structure) to the trigonal R-phase [1] and to the monoclinic B19'-phase [2], the sequence of the occurrence of these martensitic phases depending on composition and thermal and/or mechanical treatment [3]. Typical precursors of the R-phase are for example superreflections near the  $1/3$  [110] positions in transmission electron microscopy (TEM) and neutron diffraction patterns on  $\text{Ni}_{50.5}\text{Ti}_{49.5}$  and  $\text{Ni}_{51}\text{Ti}_{49}$ , respectively [4, 5]. When the reflections are locked-in at the commensurate  $1/3$  [110] positions the R-phase has formed [6]. The B19'-phase also exhibits a precursor appearing as the superreflections at  $1/2$  [110] positions in the diffraction patterns [4, 5]. Inelastic neutron scattering on  $\text{Ni}_{47}\text{Ti}_{50}\text{Fe}_3$  reveals that these reflections are related to soft  $\text{TA}_2$ -phonons at  $1/3$  [110] and at  $1/2$  [110], the B2-phase Brillouin zone boundary.

It is as well known that annealing of Ni-rich Ni-Ti alloys (quenched before from the high temperature B2-phase region) results in the formation of metastable precipitates in the sequence  $\text{Ni}_4\text{Ti}_3 \rightarrow \text{Ni}_3\text{Ti}_2 \rightarrow \text{Ni}_3\text{Ti}$  (stable) [7]. To illustrate the structural difference between the (stoichiometric) B2- and the  $\text{Ni}_4\text{Ti}_3$  phase Fig. 1 shows 27 unit cells of the B2-phase from which the  $\text{Ni}_4\text{Ti}_3$  structure can be achieved, if first only 1 Ti atom (marked with x in Fig.1) is replaced by a Ni atom and second a 2.3% contraction of the lattice along [111] is allowed because of the change in the Ni-Ni nearest neighbour coordination [8]. The bold lines in the figure represent the resulting unit cell of  $\text{Ni}_4\text{Ti}_3$ . It seems likely that in a quenched Ni-rich alloy substantial part of the substitutionally disordered B2-phase has locally already the composition of the  $\text{Ni}_4\text{Ti}_3$  precipitate. Such local „clusters“ can be considered as precursors of the precipitates. They may be the origin of a large and strongly composition dependent resistance anomaly observed by us in quenched Ni-rich Ni-Ti alloys [9].

Up to now, a detailed knowledge of the structure in the quenched austenitic phase of these Ni-Ti shape memory alloys, especially of the relevant length scale of early stage decomposition from B2 into the  $\text{Ni}_4\text{Ti}_3$  is still lacking. The present paper reports about some details of the microstructure of  $\text{Ni}_{52}\text{Ti}_{48}$  and  $\text{Ni}_{54.5}\text{Ti}_{45.5}$  alloys obtained by TEM.

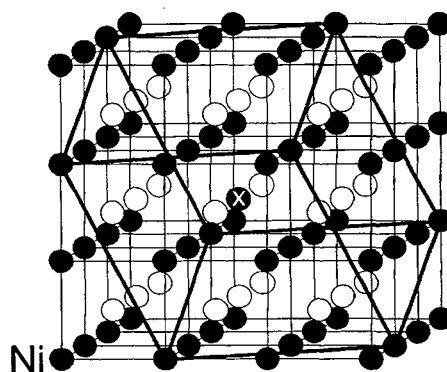
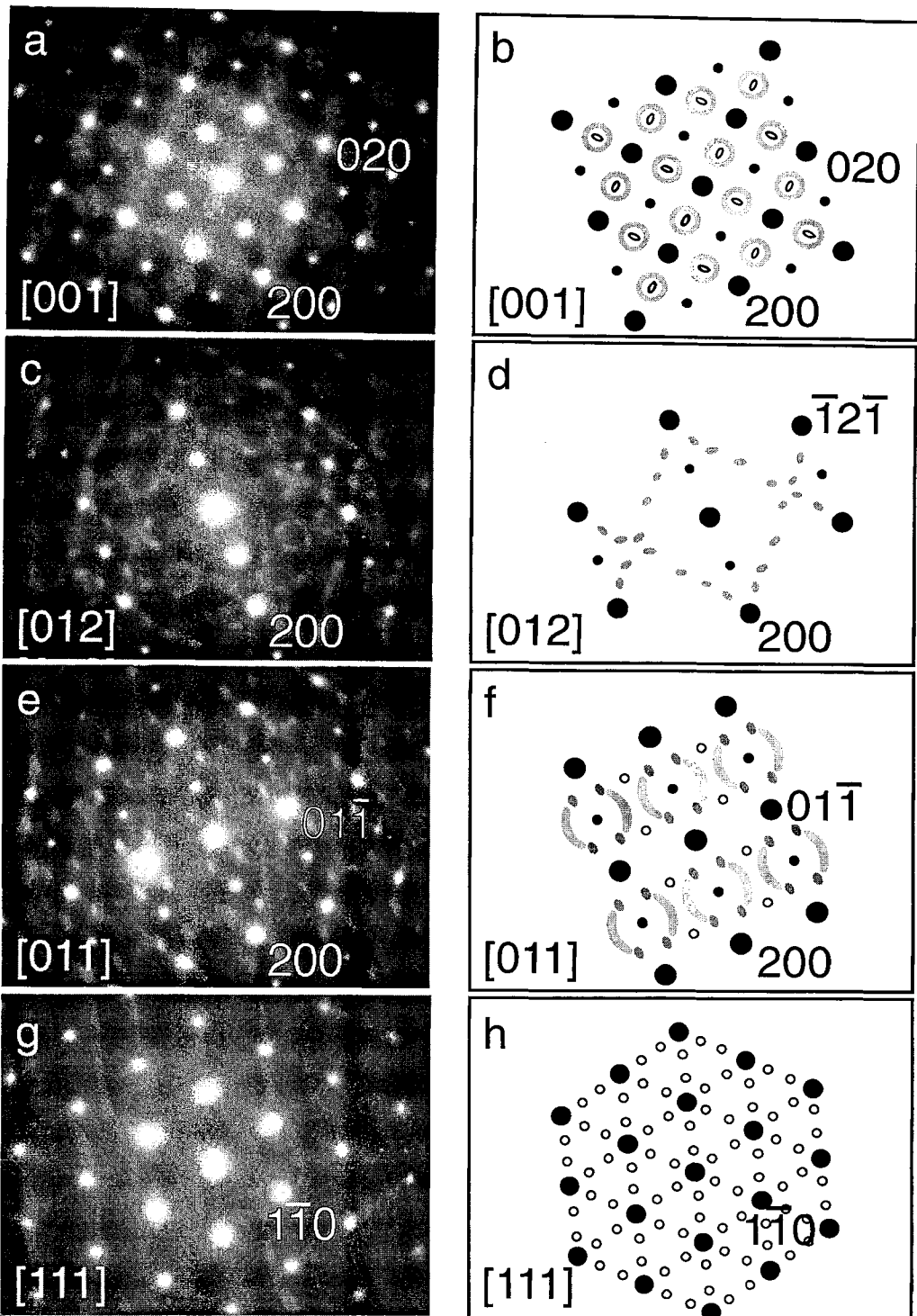


Fig. 1: Crystal structure of the  $\text{Ni}_4\text{Ti}_3$  precipitate delineated into the B2 lattice after ref. [8].



**Fig. 2:** Diffraction patterns of quenched  $\text{Ni}_{52}\text{Ti}_{48}$  of the [001] (a), [012] (c), [011] (e) and [111] (g) zone. Schematics of the diffraction patterns of [001] (b), [012] (d), [011] (f) and [111] (h) zone. Full large and small black circles represent the reflections due to the B2-phase. Open symbols represent reflections due to precursors of the R-phase and the B19'-phase, respectively. Gray symbols represent the diffuse intensity due to  $\text{Ni}_4\text{Ti}_3$  precipitates in an earlier state of formation.

## Experimental

$\text{Ni}_{52}\text{Ti}_{48}$  and  $\text{Ni}_{54.5}\text{Ti}_{45.5}$  samples were prepared by arc melting under argon atmosphere. For electron microscopy discs of 3 mm diameter (thickness 0.35mm) were spark-cut from the ingots, incapsulated in quartz tubes (500mbar Ar) and 1h solution treated at  $T=1000^\circ\text{C}$  ( $\text{Ni}_{52}\text{Ti}_{48}$ ), and  $T=1100^\circ\text{C}$  ( $\text{Ni}_{54.5}\text{Ti}_{45.5}$ ) respectively, and then quenched in ice water. Specimens were thinned using a twin-jet electropolishing system (Struers, Tenupol 3) with 8% perchloric acetic acid at room temperature. Specimens were investigated in a Phillips CM20 and Phillips CM12 TEM, respectively.

## Results & Discussion

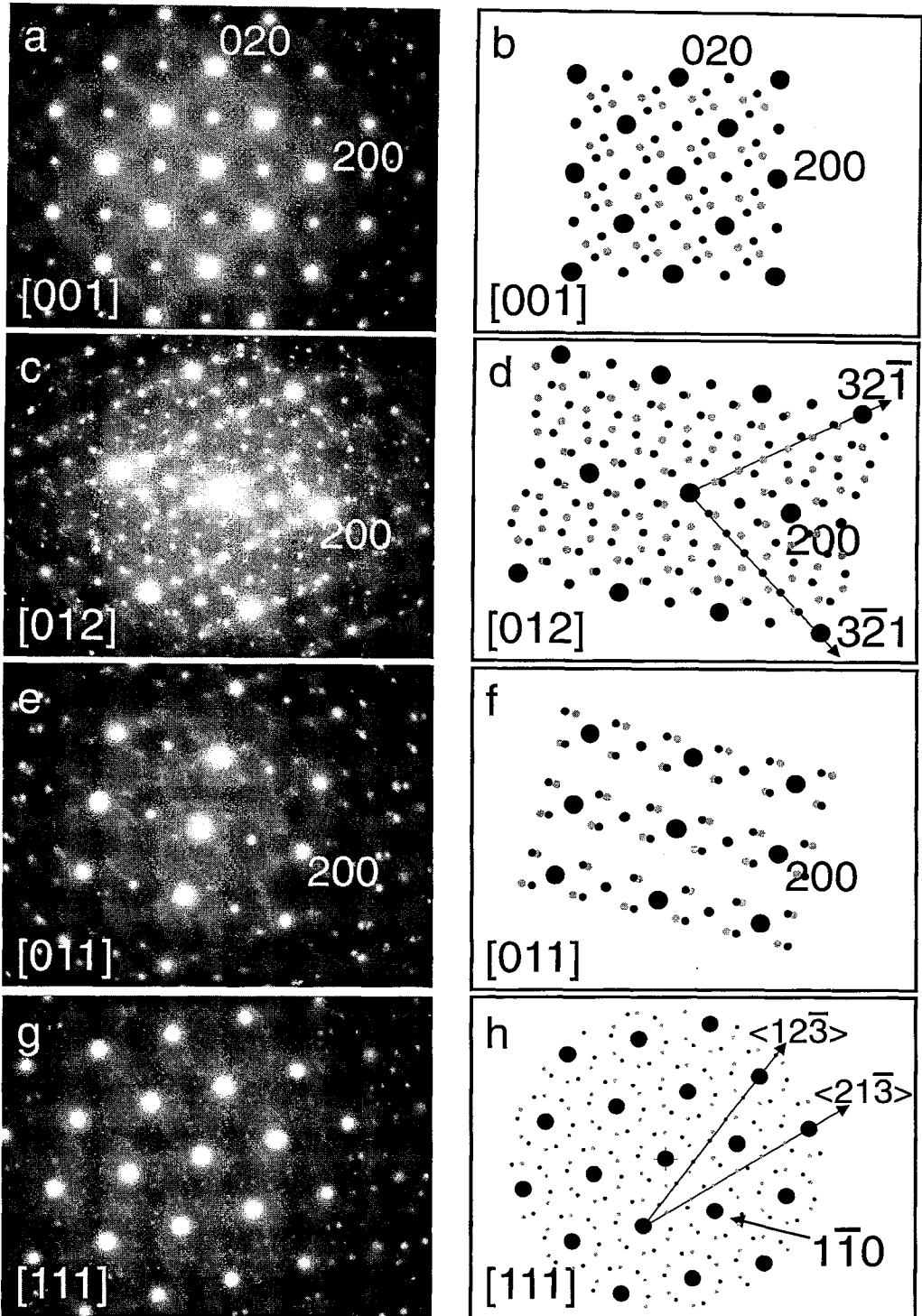
Fig. 2 shows a set of strongly illuminated diffraction patterns of the [001] (a), [012] (c), [011] (e) and [111] (g) zones for quenched  $\text{Ni}_{52}\text{Ti}_{48}$ , obtained by tilting a single grain around the [100] and the [110] axis. Figs. 2b, d, f, h schematically reproduce the main features and spots. Basic reflections are represented by large black dots, ordering reflections by small black dots. From these patterns the B2 type ordering is immediately identified by the strong ordering reflections at the  $h+k+l=2n+1$  type positions, e.g. at 100, 010 and 111. Next to these expected reflections, spots with weaker intensities are visible. Based on their structural origin, these extra intensities can be divided into two sets. A first set includes the reflections at  $1/2\langle 110\rangle$  in the [001] zone (open ellipses in Fig. 2b), at  $1/2\langle 11-1\rangle$  in the [011] zone (small open circles in Fig. 2f) and close to  $1/3\langle 1-10\rangle$  in the [111] zone (small open circles in Fig. 2h). Following the conclusions by Michal et al. [4] the appearance of this set of reflections can be explained by lattice displacement waves which are precursors of the B19'- and the R-phase. This will be discussed in more detail within a forthcoming paper.

The second set consists of reflections of more or less diffuse intensity. Under certain conditions this set develops into reflections of high intensity with particular shapes without, however, ever forming sharp reflections. In the schematic of Fig. 2 these intensity distributions are indicated by light-gray regions. When tilting through reciprocal space, most of the intensity distributions of this type are located in between the simple crystallographic zones, forming short "bars" of intensity along particular crystallographic directions. Only the [011] zone (Fig. 2e, f) reveals some strong intensities (dark gray spots) possibly belonging to this second set and located at  $1/6\langle 31-1\rangle$  positions. For the [012] zone (Fig. 2d), the 6 intensity enhancements visible between, e.g. the  $\langle 200\rangle$  and  $\langle -12-1\rangle$  reflections resemble the  $1/7\langle 321\rangle$  type superreflections of the  $\text{Ni}_4\text{Ti}_3$  structure [8].

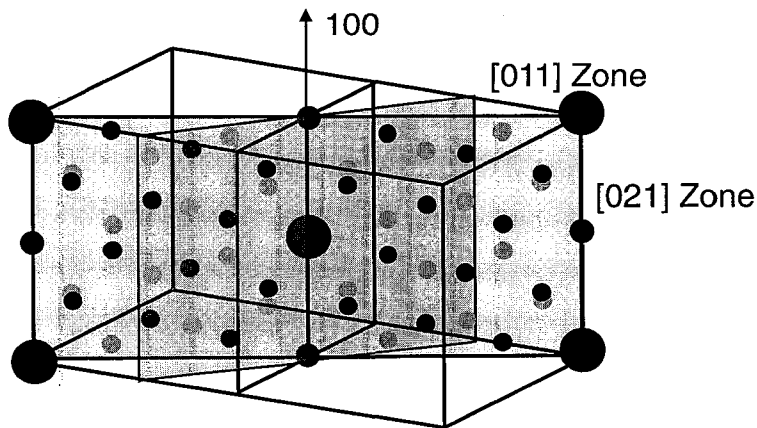
The diffuse intensities found in the two other zones [001] (2a) and [011] (2e) cannot simply explained by reflections originating from  $\text{Ni}_4\text{Ti}_3$  precipitates because this structure does not produce reflections in these zones. Assuming, however, that the  $1/7\langle 321\rangle$  type reflections are smeared out in reciprocal space (because the lateral extension of the precipitation nuclei is small), they may be identified with the diffuse intensities mainly located along the  $\langle 310\rangle$  and  $\langle 311\rangle$  directions which are close to the  $\langle 321\rangle$  directions. Contrasting to this, virtually no diffuse intensity is observed in the [111] zone (2h), containing the  $\langle 321\rangle$  type directions as well. Comparison with the results for the  $\text{Ni}_{54.5}\text{Ti}_{45.5}$  sample (see Fig. 3h below) let us conclude that the reflections are too weak to be seen in this sample. Summarizing the results of Fig. 2 we state that already in the quenched  $\text{Ni}_{52}\text{Ti}_{48}$  sample atomic groups with an ordered configuration resembling the  $\text{Ni}_4\text{Ti}_3$  precipitates on a small length scale are present.

Fig. 3 shows the diffraction patterns analog to Fig. 2 for the quenched sample  $\text{Ni}_{54.5}\text{Ti}_{45.5}$  taken at  $T=100\text{K}$ . Comparison of these diffraction patterns with those of the  $\text{Ni}_{52}\text{Ti}_{48}$  sample in Fig. 2. shows that the reflections  $1/2\langle 110\rangle$  in the [001] zone (open ellipses in Fig. 2b),  $1/2\langle 111\rangle$  in the [011] zone (open circles in Fig. 2f) and  $1/2\langle 110\rangle$  in the [111] zone (open circles in Fig. 2h) are absent in Fig. 3. Obviously in the  $\text{Ni}_{54.5}\text{Ti}_{45.5}$  alloy no precursors of the B19'- and R-phase exist. From this we infer that the quenched B2-phase of this alloy is more stabilized against the martensitic transition than the  $\text{Ni}_{52}\text{Ti}_{48}$  alloy.

Instead of diffuse intensity visible in Fig. 2 and related to  $\text{Ni}_4\text{Ti}_3$  precipitates in an early state of formation more or less well defined spots appear in Fig. 3. Furtheron, the  $1/7\langle 321\rangle$  reflections originating from two variants of the  $\text{Ni}_4\text{Ti}_3$  precipitates can be identified in all zones shown (small black and gray circles, in Figs. 3b, d, f, h). The superreflections are exactly located in the [012] and [111] zones whereas they are located only



**Fig. 3:** Diffraction patterns of quenched  $\text{Ni}_{54.5}\text{Ti}_{45.5}$  of the [001] (a), [012] (c), [011] (e) and [111] (g) zone. Schematics of [001] (b), [012] (d), [011] (f) and [111] (h) zone with superreflections of two variants of  $\text{Ni}_4\text{Ti}_3$  precipitates. Full large and medium-sized black circles represent the reflections due to the B2-phase. Small black and gray circles represent the  $1/7$   $\langle 321 \rangle$  superreflections of the  $\text{Ni}_4\text{Ti}_3$  precipitates for two variants. Arrows indicate  $\langle 321 \rangle$  directions.



**Fig. 4:** Schematics of the reciprocal lattice of the  $\text{Ni}_4\text{Ti}_3$  precipitates. All reflections of the [021] zone are shown. Only the  $1/7 \langle 321 \rangle$  reflections next to the 100 axis are visible in the [011] zone.

close to the [001] and [011] zones. To illustrate this, in Fig. 4 all the reflections of the [021] zone corresponding to the B2-phase and two variants of the  $\text{Ni}_4\text{Ti}_3$  precipitates are shown. Those superreflections which are lying close to the marked  $\langle 100 \rangle$  axis are also close to the [011] zone and therefore visible in this zone as well.

### Summary

TEM diffraction patterns of quenched  $\text{Ni}_{52}\text{Ti}_{48}$  show that the microstructure is characterized by the appearance of precursors of the B19' and the R-phase and by nuclei of  $\text{Ni}_4\text{Ti}_3$  precipitates. For the quenched Ni-rich composition  $\text{Ni}_{54.5}\text{Ti}_{45.5}$  no martensitic precursors can be found and the degree of formation of the  $\text{Ni}_4\text{Ti}_3$  precipitates is higher. Both phenomena, the martensitic precursors and the precipitates lead to a distortion of the high temperature B2-phase lattice which apparently causes the observed resistance anomaly at low temperatures. It is not yet clear which of the two structural features is more effective. Additional results and a more detailed discussion will be following in a future paper.

### Acknowledgments

The authors are grateful to T. Kakeshita (University of Osaka) for useful discussions.

### References

- [1] T. Hara, T. Ohba, E. Okunishi and K. Otsuka, *Mater. Trans. JIM* 38 (1997) 11
- [2] Y. Kudoh, M. Tokonami, S. Miyazaki and K. Otsuka, *Acta Metall.* 33 (1985) 2049
- [3] D. Treppmann, *Thermomechanical Treatment of NiTi*, VDI-Fortschrittberichte, Reihe 5, Nr. 462, VDI-Verlag, (1997)
- [4] G.M. Michal, P. Moine and R. Sinclair, *Acta Met.* 30 (1982) 125
- [5] A.I. Lotkov, S.F. Dubinin, S.G. Teplouchov, V.N. Grishkov and V.P. Scorobogatov, *J. Phys. IV* 5 (1995) C8-551
- [6] S.K. Wu and C.M. Wayman, *Acta Metall.* 37 (1989) 2805
- [7] M. Nishida, C.M. Wayman and T. Honma, *Metall. Trans.* 17A (1986) 1505
- [8] T. Tadaki, Y. Nakata, K. Shimizu and K. Otsuka, *Trans. JIM.* 27 (1986) 731
- [9] Ch. Somsen, H. Zähres, J. Kästner, E.F. Wassermann, T. Kakeshita and T. Saburi, *Mater. Sci. Engng.* A273-275 (1999) 310